

Experimental Verification of a Software for Simulation of Heating Metallic Parts in Solar Furnaces

Maria STOICĂNESCU

Transilvania University of Brasov, Romania, stoican.m@unitbv.ro

Aurel CRIȘAN

Transilvania University of Brasov, Romania, crisan.a@unitbv.ro

Mihai Alin POP

Transilvania University of Brasov, Romania, mihai.pop@unitbv.ro

Ioan CIOBANU

Transilvania University of Brasov, Romania, ciobanu.i@unitbv.ro

Abstract

Lately, experimental research has been carried out on the use of concentrated energy solar furnaces for the thermic processing of materials. On this line, at Transilvania University a software was developed for simulating the heating of metal parts in such furnaces. In a previous paper was presented the mathematical model that underpinned the realization of this software. This paper presents the results of experimental validation of this software. There are compared the heating curves of a test piece, obtained by simulation (with this software), with the heating curves obtained by experiment. The results confirmed the validity of the software. It is concluded that the software can be used to simulate on the computer the working parameters of the concentrated power flow solar furnaces for the thermic processing of some metallic parts (e.g. heat treatments in volume, surface heat treatments, melting, welding, surface coatings, etc.).

Keywords

heating simulation, solar furnaces, heat treatment, software verification, heat treatment, solar energy

1. Introduction

The sun is an inexhaustible, cheap, ecological energy source. The interest in the use of solar energy dates back to the Middle Ages. Archimedes is reminded that during the Punic War (218-202 bC) he rejected the roman attacking ships by firing them with burning bottles (possibly orientated mirrors). The first modern solar furnace was built in France in 1949 by Professor Felix Trombe. It is located in Mont Louis, in the Pyrenees.

At present, solar energy is widely used for water heating and power generation. Worldwide high power pilot installations using concentrated solar power (Parkent City - Uzbekistan, Almeria - Spain, Neuchatel - Switzerland) were built. Solar rays are concentrated in the focus of a mirror (parabolic or spherical). Items under heating are placed in the focus of the concentrating mirror. Temperatures up to 4000 °C can be achieved [4]. The disadvantage of these installations is that the surface (area) of the concentrated energy spot (and hence the energy transfer surface to the heated part) is reduced (in the order of 10-12 cm²). Instead, the specific power (W/m²) transmitted to the piece is very high (up to 6,000,000 W/m²). Research has been conducted on the use of this type of (concentrated power) furnace in industrial applications.

2. The Importance of Computer Simulation of Heating in Solar Furnaces

An area in which concentrated solar energy could be used is the thermic processing of metals.

Research is being done for the following processing:

- heat treatments in volume [2, 3, 7];
- surface heat treatments [5, 6, 7];
- surface melting and alloying[5, 6];
- thin-layer coatings [5];
- welding [3], etc.

Heat treatments of metal parts involve heating them (in entire volume or just on the surface) at high temperatures (usually up to 1300 °C - depending on the alloy and processing type). At present, the heat treatments of metal parts use energy that comes either from the combustion of classic fuels (methane gas, oil), or from the conversion of electrical energy into heat (through resistors, induction, electric arc). Lately the use of solar energy is being explored for this purpose.

For industrial applications, it is necessary to use the solar energy under conditions corresponding to the requirements of the processing technologies. The heating temperature depends on the alloy type and the heat treatment applied. The distribution of temperature in the piece volume is also very important. For heat treatments in volume, the technological temperature must be as uniform as possible in the whole volume. In the case of surface treatments, the temperature must be high only in a superficial layer (usually in thickness of millimeters) and in the remaining volume the temperature must be kept below certain values. Studies on the use of solar energy for the thermic processing of metals have been carried out since the middle of the last century [4]. The tests were conducted on different materials (steels, cast iron, non-ferrous alloys). They aimed to adapt the constructive features of solar furnaces for the experimented processes [3, 5]. Research was conducted on small samples (with a diameter between 20-45 mm and lengths between 1.5-100 mm). Attempts have demonstrated the possibility of treatments such as superficial hardening and volume hardening in such furnaces. It was highlighted the possibility of obtaining the desired structures and properties in the treated materials. It has also been emphasized that (in the case of small parts) the most important advantage of this type of furnaces, namely high heating speed of the parts (due to the very high specific power), can be realized.

The thermic processing of metal parts in solar furnaces requires setting and adjusting the working parameters of solar installations according to their particularities and the requirements of the technologies. For this purpose it is necessary to establish correlations between the geometric and dimensional parameters of the parts, the technological parameters for the heat treatment (the required temperature, the heated volume, the heating speed, the heating time, the cooling mode - parameters which depend on the final properties of the parts); respectively, the operating parameters of the solar furnace (maximum specific power in the focus of the installation, change of the incident power on the part during heating, total heating time, cooling way, etc.). Establishing such dependencies is absolutely necessary for adjusting the operation of the solar installation and for the reproducibility of the results.

The setting of the working parameters of the solar installations correlated with the technological process and with the type-dimensional parts can be done in two ways;

- by experimental research; the working parameters of the solar furnace are progressively changed and the effects of the processing are determined (structure, properties - hardness, mechanical resistance, etc.);
- by computer simulation of the heating of the parts in the solar furnace; the simulation conditions are progressively modified, finally choosing the work variant that induces in the part the temperature field required for the applied thermic processing.

The experimental method has disadvantages:

- large number of experiments (under the condition of changing the installation's operating parameters);
- difficulties of punctual measurement of some working parameters;
- considerable work for the preparation of samples (specimens, metallographic samples, etc.);
- a large number of tests to determine the structure and properties;
- long working time;
- high labor and energy consumption;- high costs.

The simulation method has the following advantages [8-15]:

- the values of all installation operating parameters can be easily changed,
- information on process processing parameters (temperature, heating and cooling speed, temperature gradient, etc.) can be obtained for any point in the piece;
- no test parts, work devices, apparatus for determining structure and properties are required;
- reduced working time;
- low number of experiments to validate the results.

For the simulation method to highlight these advantages it is necessary to meet the following conditions:

- making of mathematical models and software to reproduce as accurately as possible the physical and chemical phenomena specific to processing;
- the software validity assumptions (the simplifying assumptions of the mathematical model on which the software is based) to be known in order to evaluate any errors (often hypotheses of mathematical models are not known, being considered a secret by the software developers);
- a complete database on the physicochemical characteristics of the materials is needed;
- finally, an experimental verification of the working variant adopted for the purposes of validating the simulation results and for industrial application under reproducible conditions.

Recently, several experimental researches have been initiated to adapt the various heat treatment technologies of metal parts to solar furnaces. They aimed to establish the working parameters of the solar furnace for various industrial applications. At Transylvanian University of Brasov in collaboration with other universities in Europe (Spain, France), there have been addressed research projects for the use of solar furnaces for the thermic processing of metal parts. Tests have been carried out on heat treatments and superficial thin-layered coatings of metal parts. Experimental research was carried out at the CIEMAT-PSA solar center in Almeria, Spain, on the vertical SF5 solar furnace.

More trials and promising results were obtained in the case of the (volume or surface) hardening of the steel parts. The hardening aims to obtain (in all volume or surface layer) steel parts with a martensite structure with hardness and high wear resistance. For this purpose, the respective area (the entire volume or superficial layer) of the parts is heated very quickly at high temperatures (above 780 °C) depending on the chemical composition of the steel. Then the parts are quickly cooled (in water or oil) in order to obtain a hard, wear-resistant martensite structure in this layer.

3. Purpose of the Paper

At the Transylvania University of Braşov, a software was developed to simulate the heating of metal parts in solar furnaces (SIM-3D-Solar-1). The software uses a mathematical model with finite differences. It reproduces the thermophysical processes in the heat-treated part, including phase transformations. The mathematical model and the software were presented in a previous paper [15]. The purpose of this paper is to experimentally verify the results obtained with this software regarding the simulation of heating of metal parts for heat treatments. Validation of the software will allow it to be later used to simulate the working conditions of the solar furnace for heat treatment (superficial hardening, hardening in volume, etc.) of the various parts customized by geometry, dimensions, type of alloy.

4. Working Mode

Validation of the software was done by comparing the results obtained by simulation with the results obtained by experiment. A steel sample was heated in a concentrated power solar furnace. The temperature evolution was measured at various points with thermocouples and pyrometers. Then the heating of the sample was simulated in the experimental conditions (working parameters of the solar furnace and geometric and thermophysical characteristics of the sample piece). The heating curves were simulated for the points where the experimental temperature was measured. Finally, the results obtained by simulation were compared with those determined experimentally, thus establishing conclusions regarding the validity of the software to be used for simulation.

5. The Solar Furnace Used in the Experiment

The experimental research was carried out on the vertical SF5 solar furnace, from the CIEMAT Solar Platform - Almeria, Spain [1]. The functional working diagram of this furnace is shown in Figure 1. It is a solar furnace with vertical flow of radiant energy. The solar radiation falling on the mirrors of a heliostat (with a large surface) is directed towards the mirrors of a radiant flow concentration system. The concentrator is parabolic or spherical and reflects the rays in the form of a spot towards the focus. The parts subjected to heating are positioned in the focus. Here they are placed on a copper support plate placed in turn on a refractory ceramic support plate. The advantage of vertical furnaces in relation to solar furnaces with the horizontal flow axis is that the metallic samples subjected to heating can be

placed on the support plate without fixing devices. The total maximum power of the oven is 5 kW. The incident power in the focal plane (on the surface of the samples) can be adjusted by means of a damper with flaps. By rotating the flaps, the flux intensity reflected by the heliostat to the concentrator can be adjusted between zero and the maximum value. The maximum furnace power corresponds to the maximum opening of the flaps. The theoretical specific power in the focus is maximum on the incident flow axis and has the value of $P_{\text{max}} = 17,400,000 \text{ kW/m}^2$. This occurs for solar power incidental to the ground (on the surface of the heliostat) $P_{\text{sol}} = 1000 \text{ kW/m}^2$. The specific power in the focus plane power decreases (in lateral direction beside the center of the focus) after a Gauss curve. At a 2.5 cm deviation from the center of the focus plane, the theoretical specific power decreases to about 10000 kW/m^2 , and at a distance of 5 cm the theoretical specific power drops below 2000 kW/m^2 .

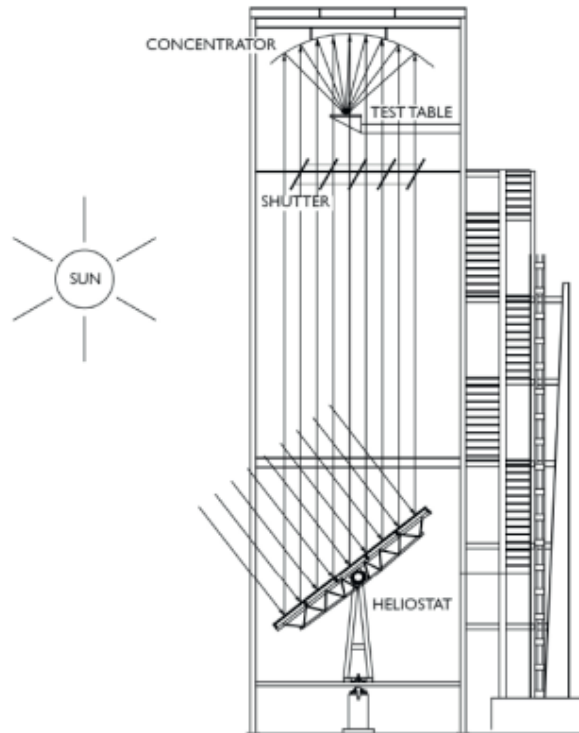


Fig.1. Functional design of vertical solar furnace SF5 (Solar Platform of Almeria, Spain) [1]

The concentrator consists of a plurality of hexagonal planar faces (with the hexagon side of 25 cm). Their centres are placed on the surface of a paraboloid with a focal length of 2 m. As a result, the actual reflective surface of the concentrator is not perfectly parabolic. Therefore, the actual power incident in the focal plane of the furnace is smaller than the calculated theoretical power for a perfectly parabolic surface of the concentrator. Experimental radiometric measurements have shown that the maximum incident power (at the maximum aperture, 100% of the damper's flaps) in the center of the furnace's focal plane (for $P_{\text{sol}} = 1000 \text{ kW/m}^2$) is 6380 kW/m^2 . For smaller apertures of the damper, the power specified in the center of the focal plane decreases as shown in Table 1.

Table 1. Specific power measured in the focal plane (focal length $f = 2 \text{ m}$)

No.	Damper's aperture	Specific power in the center of the focal plane
u.m.	%	kW/m^2
1	10	589
2	20	1172
3	40	2396
4	60	3563
5	80	4922
6	100	6380

6. Working Conditions for the Experiment

The experiment for software verification was performed on metallic samples made of non-alloyed 1.1730 steel with a chemical composition of 0.45% C; 0.30% Si; 0.70% Mn. This steel has the heating temperature for heating in volume TC = 840-860 °C. After heating at the hardening temperature the parts have to be cooled in water. Parallelepiped samples of length \times width \times thickness = $L \times B \times H = 33 \times 25 \times 10$ mm were used. Two thermocouples were assembled for measuring and recording the temperature in the metallic sample. The sample's sizes and the position of the points (T1, T2) in which the temperature was measured and recorded by thermocouples is shown in Figure 2. The temperature evolution was also measured using an optical pyrometer. It measured and recorded the temperature at the point situated in the center of the top surface of the sample (at point O on the axis of the spot, see Figure 2). The sample was placed in the focus of the furnace inside a glass working room as shown in Figure 3. An antioxidant protective gas was introduced into the working room. The steel sample was placed on a 10 mm thick copper plate, and the plate was placed on a 5 mm thick refractory ceramic plate. The heating time was $t = 23.3$ minutes. After heating, the piece was suddenly cooled in water for hardening.

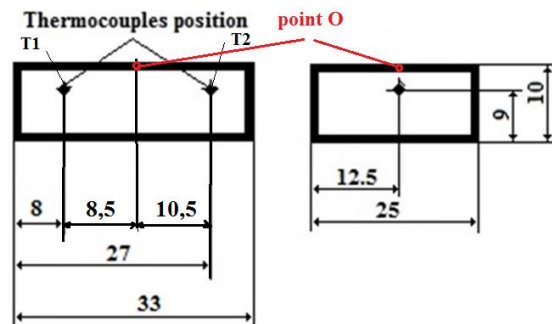


Fig. 2. Experimental metallic sample heated inside the solar furnace

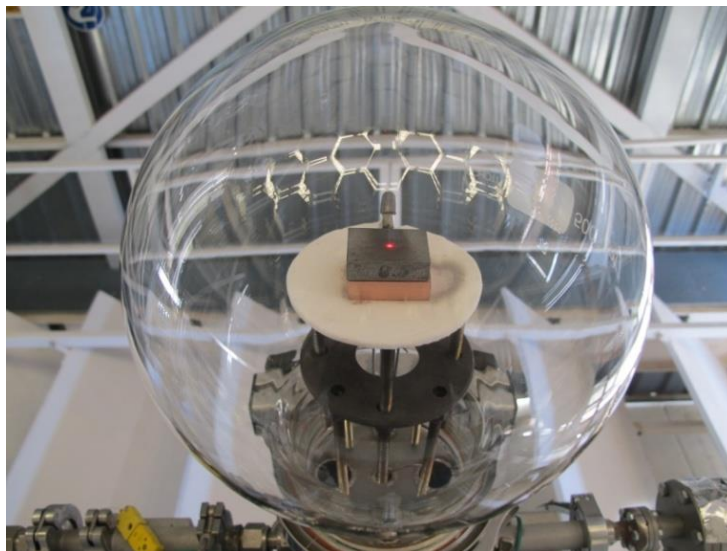


Fig. 3. Position of the metallic sample inside the heating room on the focal plane of the solar furnace

6. Experimental Results

Figure 4 graphically represents the values of the solar furnace's working parameters during the experiment (specific solar power incident on the heliostat, the aperture of the damper's flaps) as well as the temperatures measured by the thermocouples and the pyrometer. To obtain an approximate steady-speed heating, the flaps of the damper have been opened progressively between 5-23%. The power of incident solar radiation (captured by the heliostat) was on average $P_{sol} = 975$ W/m². The experimentally recorded heating curves show the following results:

- maximum temperature measured by the two thermocouples:
 $T1_{max_exp} = 935\text{ }^{\circ}\text{C}$ and $T2_{max_exp} = 920\text{ }^{\circ}\text{C}$;
- heating time $t = 23.3$ minutes;
- average heating speed $v_{med_i_exp} = 0.62\text{ }^{\circ}\text{C/s}$.
- the maximum temperature measured by the optical pyrometer at point O (center of the upper surface) $T_{max_pir} = 1185\text{ }^{\circ}\text{C}$.

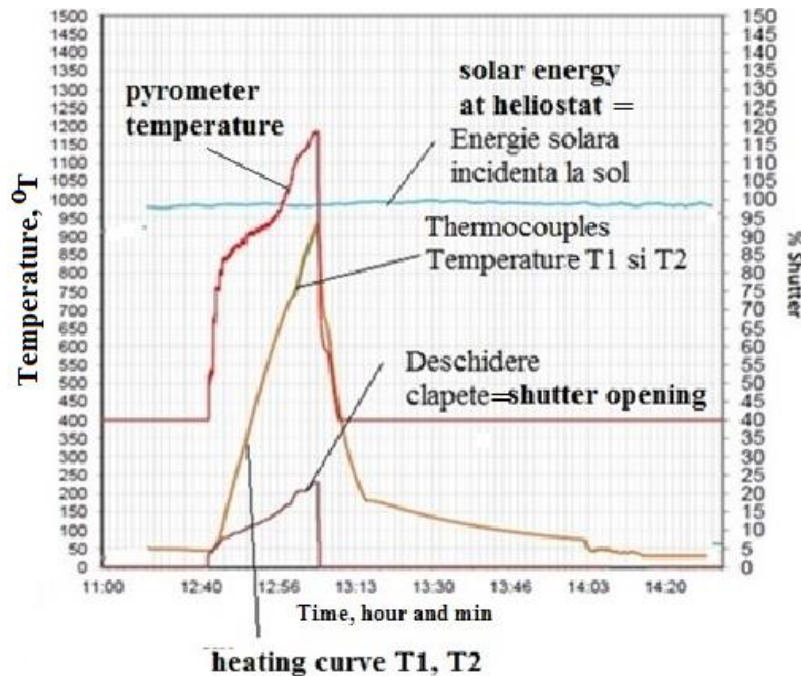


Fig. 4. Experimental results (flaps' opening depending on time and the measured temperatures by T1 and T2 thermocouples and by pyrometer)

It is noted that the temperature measured by the optical pyrometer (at point O) is higher than the one measured by the thermocouple. The explanation is:

- different position of temperature measurement points (T1 and T2 for the thermocouple and O for pyrometer); the thermocouples show the temperature at 1.5 mm below the surface of the piece, T1 at a lateral distance of 8.5 mm in relation to the axis and respectively T2 at 10.5 mm, while the pyrometer shows the temperature at the point O located just on the surface of the piece, in its center;
- the temperature measured by the thermocouple may be influenced (to a certain extent) by the perfection of the thermocouple-sample contact (contact pressure, contact surface)
- measurement errors of the temperatures by thermocouple in relation to the pyrometer (caused by thermophysical characteristics of the thermocouple materials and by the time required to equalize the sample - thermocouple temperature).

The heating curves experimentally recorded by the two thermocouples show a slow of heating in the temperature range 720-740 °C. This corresponds to the perlite-austenite structural transformation of the steel with 0.45 °C. The ferrite + perlite structure turns into austenite by heat absorption. In the case of the curve recorded by pyrometer at point O, this transformation takes place at higher temperatures (840-930 °C). The cause is the higher heating rate at point O in relation to the T1 and T2 points. At higher heating rates the beginning of the perlite - austenite transformation (point Ac1) moves to higher temperatures due to the incubation period (inertia) of structural transformations.

7. Results Obtained by Simulation

In the second part of the research, simulation of heating was performed using the software developed at Transilvania University (SIM-3D-SOLAR-1) [15].

The assembly sample (steel) - support plate (copper plate + ceramic) subjected to heating was divided into cubic volume elements with the side $\Delta = 1$ mm as shown in Figure 5. The time step for determining the temperature evolution in the sample points was $t = 0.0015$ seconds. The heat transfer scheme underlying the mathematical model is shown in Figure 6. The simulated temperatures represent the average temperature, momentary temperature of the volume elements (1 mm side) corresponding to the peak position of the two thermocouples.

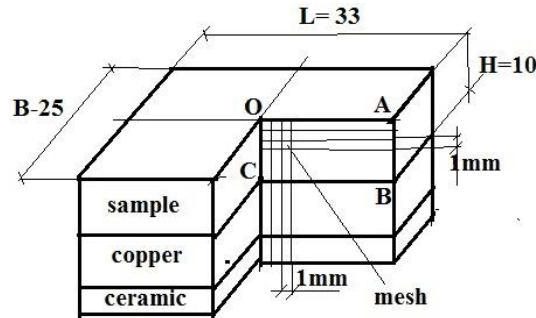


Fig. 5. Division scheme of sample - support system for simulation of heating

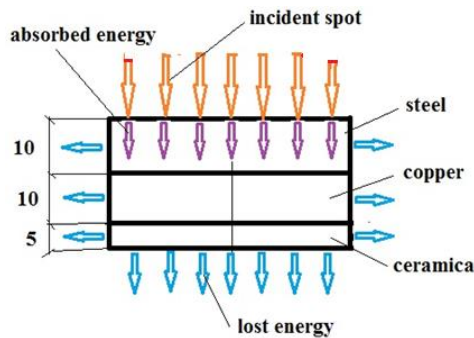


Fig. 6. The scheme of the mathematic model for simulation

One of the problems of computer simulation of heating metal parts in solar furnaces (and generally of thermic processes in solar installations) consists in knowing the value of the solar energy absorption coefficient on the surface of the heating element. The absorption coefficient of the radiation is not known precisely. The value of this coefficient depends on the type of material, processing of the part's surface, surface temperature, radiation frequency. Its value changes during heating. The literature provides indicative values. These are included in a wide range (0.1 - 0.97) as shown in Table 2. For example, for steel parts (in case of the part subjected to heating in the presented experiment) we have values of $\text{Ca} = 0.7-0.9$ for surfaces, for steel oxidized at 600°C and $\text{Ca} = 0.1$ for polished steel surfaces. For higher temperatures (over 600°C no values are given).

Table 2. Values of the emissivity coefficient - absorption for steel surfaces

No.	Material	Value	Reference
1	Cold-rolled steel	0.7-0.9	[16]
2	Polished steel	0.1	[16]
3	Polished steel	0.07	[17]
4	Steel oxidized at 600°C	0.79	[17]
5	Plate steel laminate	0.66	[17]
6	Raw steel plate	0.94-0.97	[17]

Hypotheses to be considered for simulation:

- progressive opening of the damper's flaps between 5-23% (according to the experimental curve in Figure 4);

- the sample placed on the copper plate, on a refractory ceramic plate;
- the incident specific power of the spot on the upper surface of the sample was considered as follows: in the central area (8 mm radius) an average $Q_{in1} = 6,000,000 \text{ W/m}^2$, and for the rest of the surface a mean power $Q_{in2} = 5,500,000 \text{ W/m}^2$ taken into account the actual incident force on the ground and the focal plane of the concentrator during the experiment);
- the initial area of the samples has been polished;
- for the range of 50 -720 °C it was considered that the radiation absorption coefficient on the surface of the sample increased linearly between $Ca = 0.25-0.57$ (it was taken into account that the initial surface of the samples was polished, and that while the temperature increases a change of color of the surface takes place, which leads to increased absorption, up to 720 °C);
- at temperatures between 720 and 850 °C when the surface of the sample turns red, the absorption coefficient of the solar radiation was considered $Ca = 0.7$, then in the range 850-940 °C (when the part becomes incandescent) was considered $Ca = 0.55$;
- average heat exchange coefficient equivalent (convection + radiation) sample - ambient on side and bottom surfaces, $\alpha_{ex} = 27 \text{ W/m}^2\text{K}$;
- the contact between the steel sample, the copper support plate and the ceramic plate is perfect;
- heating time $t = 23.3$ minutes (the same as for the experiment).

By simulation the temperature evolution was determined in all discretized volume elements in the sample-support system (temperature map at various times, local heating speed, temperature distribution in various directions at any time).

Figure 7 shows the heating curves obtained by simulation for the volume elements corresponding to the tip of the thermocouples (points T1 and T2).

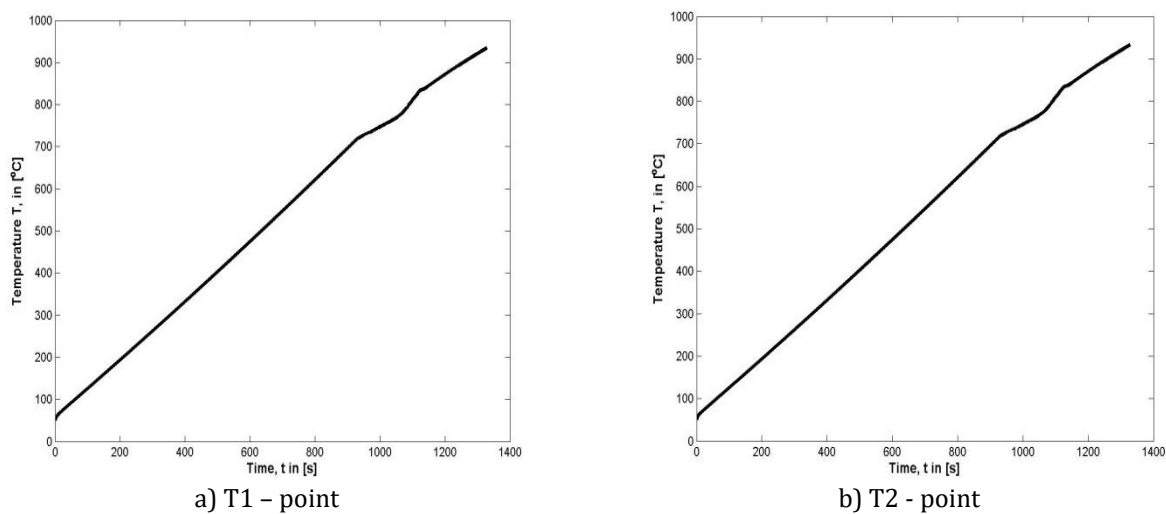


Fig. 7. Temperature evolution in T1 and T2 points (by simulation)

8. Conclusions

In Figure 8, these curves (curves determined by simulation) are overlapped (in the same graph) over the experimentally recorded heating curves (for T1 and T2 points). It is noted that the simulated curves are very close to those determined experimentally by thermocouple measurement. (Figure 8). This leads to the conclusion that the experiment confirms the simulation. As a result, the software can be used with confidence in industry and research for technological process design.

8. Other Results

Below there are other results obtained by simulating the sample heating from Figures 2, 5 and 6. Table 3 gives the temperature values of all volume elements with the side of $\Delta = 1 \text{ mm}$ of the OABC section of the sample (Figure 5) at time $t = 23.3 \text{ min}$. In Figure 9, based on the values in this table, is represented the isotherm map (temperature distribution) in the AOBC section in the support -sample system at time $t = 23.3 \text{ min}$.

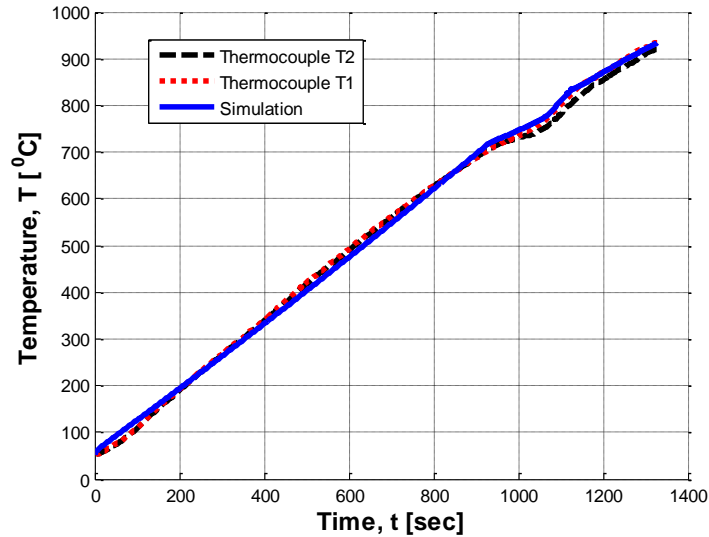


Fig. 8. Temperature evolution in T1 and T2 points (by simulation and experiment)

Table 3. Simulated results - temperature (in °C) in the volume elements of the part in OABC plan (Figure 5) at time t = 23.3 min

Temperature in OABC section, in °C

C_j = Column number (j=1÷17 = Distance from the sample axis (OC) in mm)

	C1	C2	C3	C4	C5	C6	C7	C8	C9	C10	C11	C12	C13	C14	C15	C16	C17
O	Pyrometer point																A
L1	941.1	941.0	941.0	940.8	940.6	940.3	939.9	939.4	938.7	938.2	937.6	937.1	936.5	935.9	935.3	934.6	933.9
L2	936.6	936.6	936.5	936.3	936.1	935.8	935.5	935.1	934.5	934.0	933.5	933.0	932.5	931.9	931.3	930.6	929.8
L3	932.3	932.3	932.2	932.0	931.8	931.6	931.3	930.9	930.5	930.0	929.6	929.1	928.6	928.0	927.4	926.7	926.0
L4	928.2	928.2	928.1	928.0	927.8	927.6	927.3	927.0	926.6	926.2	925.8	925.3	924.8	924.3	923.7	923.1	922.4
L5	924.3	924.3	924.2	924.1	923.9	923.7	923.5	923.2	922.9	922.6	922.2	921.8	921.3	920.8	920.2	919.6	918.9
L6	920.6	920.6	920.5	920.4	920.3	920.1	919.9	919.6	919.4	919.1	918.7	918.4	918.0	917.5	917.0	916.4	915.7
L7	917.0	917.0	916.9	916.9	916.7	916.6	916.4	916.2	916.0	915.7	915.5	915.1	914.8	914.4	913.9	913.3	912.7
L8	913.6	913.6	913.6	913.5	913.4	913.3	913.1	913.0	912.8	912.6	912.3	912.1	911.8	911.4	911.0	910.5	909.9
L9	910.4	910.4	910.3	910.3	910.2	910.1	910.0	909.9	909.7	909.6	909.4	909.2	908.9	908.7	908.3	907.9	907.4
L10	907.2	907.2	907.2	907.2	907.1	907.0	906.9	906.9	906.8	906.7	906.5	906.4	906.2	906.1	905.9	905.6	905.3
C																	B

Li=Ligne number (i=1-10 = Distance from the upper border (OA) in mm)

Figure 10 shows the temperature variation of the volume element located at the center of the top surface of the part (point O - Figure 6). By comparing this curve with the experimental curve (Figure 4) measured with the optical pyrometer, relative differences are observed. This can be explained by the fact that the temperature measured by pyrometer is the surface temperature, while the temperature displayed by the simulated curve is the average temperature of a discretized cubic volume with the side of 1 mm. The maximum temperature showed by the optical pyrometer (in point O, Figure 5) is $T_{max_pir_0} = 1185\text{ °C}$ (Figure 4), while the maximum temperature obtained by simulation in the cell (of volume with side of 1 mm) corresponding to this point is $T_{max_sim_0} = 941.1\text{ °C}$.

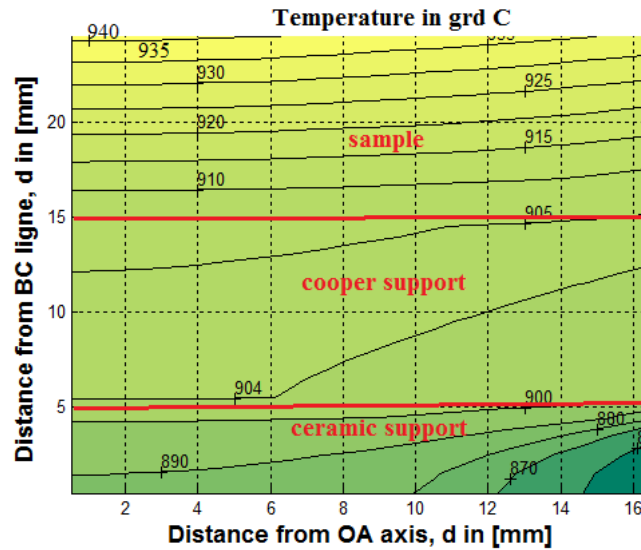


Fig. 9. Temperature map (isotherm lines) by simulation, in °C inside OABC cut - by sample - support assembly at time $t = 23.3$ min

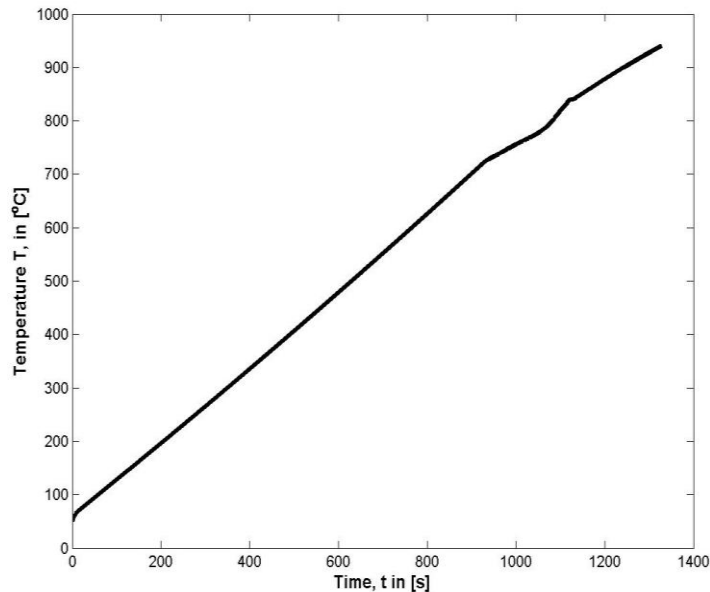


Fig. 10. Heating of the element located in the center of top side (layer with 1 mm thickness) of the sample (in point O)

The relatively large difference is explained by the fact that the pyrometer shows the temperature on the surface of the piece, while the simulation calculates the average temperature of a volume element with the side $D = 1$ mm placed at the point O. To simulate more exactly the temperature measured by the optical pyrometer (temperature in point O on the sample surface) it would be necessary to perform a simulation under conditions similar to the heating of the top surface of the sample. Thus, the transformation interval of the perlite + ferrite structure into austenite should be $840 - 930$ °C (according to Figure 4, which corresponds to a higher heating rate). It would also be necessary to make a discretization of the volume with a very small mesh (e.g. $\Delta = 0.01$ mm). This is to obtain a temperature as close as possible to the temperature of the top face of the sample. The smaller the mesh of the discretization network, the more precise is the temperature measured by the optical pyrometer on the sample surface represented by the simulated temperature for the surface layer. A very small step of discretization results in very high simulation times. For example, a twice reduction in the volume discretization step, results in an increase in the simulation time of 32 times. A splitting step of $\Delta = 0.1$

mm would require (in the case of a personal computer) simulation times of the order of 30,000 hours (which is hard to do in practice).

Figure 11 shows the temperature distribution on the OA line in the superficial layer of the sample (1mm thick) at time $t = 23.3$ min. The temperature on this line (which corresponds to the longitudinal axis of the upper surface of the sample) is relatively uniform. The difference between the temperatures of point O (center of surface) and that of point A (surface edge) is only 33.7 °C (Table 3). Figure 12 shows the temperature distribution on the vertical axis of the sample-support system (line OC - Figure 5) at time $t = 23.3$ min. This figure highlights the relatively high heating of the copper and ceramic plates. The values in Table 3 and Figures 9 to 12 show that the steel sample is heated virtually throughout the entire volume. The temperature in the sample used in the experiment has acceptable uniformity for the heat treatment of hardening in volume. Thus the working conditions applied in the experiment are recommended for heat treatment in volume (hardening) of steel parts of dimensions comparable to the dimensions of the sample. The temperature in the piece can be even more uniform through a short (post-heating) hold before putting it into the cooling medium (water or oil). However, the heating conditions applied in this experiment are not recommended for superficial hardening. This is why further simulation studies are required to determine the working parameters of solar furnaces customized for heat treatments (superficial hardening, thin-layers coatings, etc.), and also for parts with different geometry and dimensions. It is also necessary to continue the research for experimental validation of the software for heating metal parts in solar furnaces.

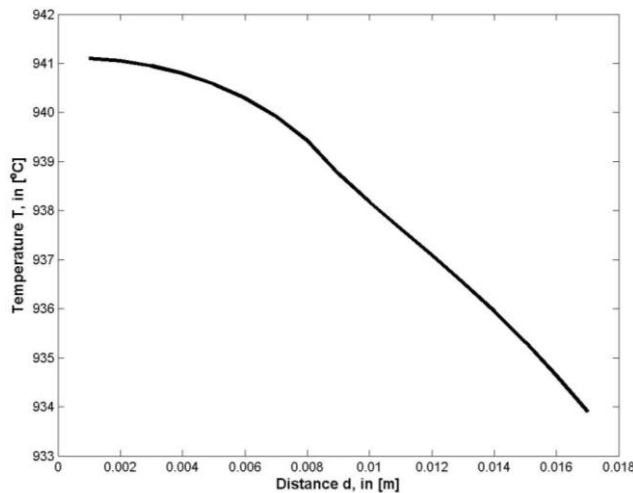


Fig. 11. Temperature in the superficial uplayer (with 1 mm thickness) of the sample (on OA line) at time $t = 23.3$ min

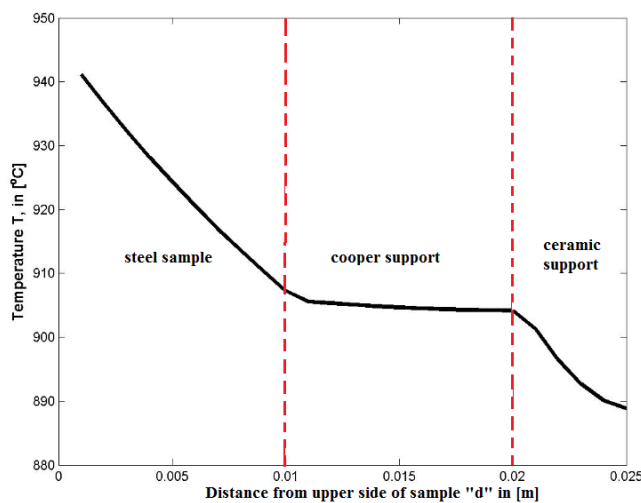


Fig. 12. Temperature on the vertical axis of part - support assembly (on OC line) at time $t = 23.3$ min

References

1. Rodríguez J., Cañadas I., Zarza E. (2014): *PSA vertical axis solar furnace SF5*. Energy Procedia, ISSN: 1876-6102, Vol. 49, p. 1511-1522, doi: 10.1016/j.egypro.2014.03.160, <https://core.ac.uk/download/pdf/82238363.pdf>
2. Llorente J., Vázquez A.J. (2009): *Solar hardening of steels with a new small scale solar concentrator*. Materials Chemistry and Physics, 118 (1), p. 86-92, <https://doi.org/10.1016/j.matchemphys.2009.07.008>
3. Karalis D.G., Pantelis D.I., Papazoglou V.J. (2005): *On the investigation of 7075 aluminum alloy, welding using concentrated solar energy*. Solar Energy Materials & Solar Cells, ISSN: 0927-0248, Vol. 8, is. 2, p. 145-163, <https://doi.org/10.1016/j.solmat.2004.07.007>
4. Sarver T., Al-Qaraghuli A., Kazmerski L.L. (2013): *A comprehensive review of the impact of dust on the use of solar energy: History, investigations, results, literature, and mitigation approaches*. Renewable and Sustainable Energy Reviews, Vol. 22, p. 698-733, <https://doi.org/10.1016/j.rser.2012.12.065>
5. Pitts J.R., Stanley J.T., Fields C.L. (1990): *Solar Induced Surface Transformation of Materials*. In: *Solar Thermal Technology-Research-Development and Applications*, B.P. Gupta & W.H. Trangott, (Eds.), Hemisphere Publishing Corporation, ISBN 978-1560320951, p. 459-470, New-York, USA
6. Vázquez A.J., Rodríguez G.P., de Damborenea J. (1991): *Surface Treatment of Steels by Solar Energy*. Solar Energy Materials, ISSN: 0165-1633, Vol. 24, is. 1-4, p. 751-759, [https://doi.org/10.1016/0165-1633\(91\)90108-W](https://doi.org/10.1016/0165-1633(91)90108-W)
7. Rodríguez G.P., López V., de Damborenea J.J., Vázquez A.J. (1995): *Surface transformation hardening of steels treated with solar energy in central tower and hliostat field*. Solar Energy Materials and Solar Cells, ISSN: 0927-0248, Vol. 37, is. 1, p. 1-12, [https://doi.org/10.1016/0927-0248\(94\)00169-S](https://doi.org/10.1016/0927-0248(94)00169-S)
8. Soporan V., Constantinescu V. (1995): *Modelarea la nivel macrostructural a solidificării aliajelor (Macrosolidification Modelling of alloys solidification)*. Editura Dacia, ISBN: 973-35-0526-9, Cluj-Napoca, Romania (in Romanian)
9. Soporan V., Constantinescu V., Crişan M. (1995): *Solidificarea aliajelor, preliminarii teoretice (Solidification of Alloys, Theoretical Preliminaries)*. Editura Dacia, ISBN 973-97041-1-5, Cluj-Napoca, Romania (in Romanian)
10. Soporan V., et al. (2010): *Modelarea matematică a proceselor care au loc la turnarea pieselor metalice (Mathematical Modelling of the Process from Metallic Casting)*. Editura Casa Cărţii de Ştiinţă, ISBN 978-973-133-059-4, Cluj-Napoca, Romania (in Romanian)
11. Soporan V., Vamoş C., Pavai C. (2003): *Modelarea numerică a solidificării (Numerical Modelling of Solidification)*. Editura Dacia, ISBN 973-35-1645-7, Cluj-Napoca, Romania (in Romanian)
12. Monescu V. (2010): *Realizarea unui program 3D pentru simularea solidificării pieselor turnate (3D Software for the simulation of castings solidification)*. PhD thesis, Transilvania University of Brasov, Romania (in Romanian)
13. Ionescu D. (2014): *Simularea solidificării pieselor turnate din aliaje cu solidificare în interval de temperatură (Computer Simulation of the Solidification of Castings from Alloys Solidifying within a Temperature Interval)*. PhD thesis, Transilvania University of Brasov, Romania (in Romanian)
14. Ionescu I.C. (2015): *Cercetări privind simularea solidificării pieselor turnate cu simetrie de rotație (Researches Regarding the Solidification Simulation of Casting with Rotational Symetry)*. PhD thesis, Transilvania University of Brasov, Romania (in Romanian)
15. Ciobanu I., Stoicănescu M., Munteanu S.I., Monescu V. (2018): *Mathematical Model and Soft for the Heating Simulation of Metallic Parts in Solar Furnaces*. RECENT, ISSN 1582-0246, vol. 19, no. 1(54) p. 19-36, <https://doi.org/10.31926/RECENT.2018.54.019>
16. <https://www.lechpol.ro/char/MIE0127.pdf>
17. <http://www.intercontrol.ro/Automatizari/EMISIVITATEADIVERSELORMATERIALE.htm>

Received: 27 August 2018. Accepted: 28 September 2018